ANALYSIS OF STEADY-STATE HEAT DISSIPATION IN SHORT HORIZONTAL RECTANGULAR FIN ARRAY

Vilson Altair da Silva, altairwayne@gmail.com
Lorenzo Alfonso Caliari de Neves Gomes, gomeslorenzo@gmail.com
Carlos Adriano Corrêa Ribeiro, cadrianocr@unifei.edu.br
Ana Lúcia Fernandes de Lima e Silva, alfsilva@unifei.edu.br
Sandro Metrevelle Marcondes de Lima e Silva, metrevel@unifei.edu.br

Universidade Federal de Itajubá - UNIFEI, Instituto de Engenharia Mecânica – IEM, Laboratório de Transferência de Calor – LabTC, Av. BPS, 1303, Bairro Pinheirinho, CEP 37500-903, Caixa Postal 50, Itajubá, MG, Brasil

Abstract. *In this work the process of heat transfer by natural convection was analyzed in rectangular finned heatsinks for different geometrical configurations. To study these configurations, different heatsinks were manufactured by varying the geometrical parameters fin spacing, height and number of fins. One essential parameter to be studied in heatsinks is the determination of the mean convection heat transfer coefficient, $\bar{h}$. In order to obtain $\bar{h}$, heatsinks were heated uniformly in their bottom surfaces and, through a system of data acquisition, the temperatures of the base and the top of the fin were measured in each heatsink. Several values of $\bar{h}$ were obtained over a temperature range between 20°C and 120°C. The results were compared with results obtained from empirical correlations found in literature. The results of $\bar{h}$ presented differences smaller than 5% for some of the heatsinks. The temperature on the top of the fin was compared with the temperature obtained by numerical and analytical solutions. Furthermore, the temperature field in function of time was calculated numerically by using the commercial software ANSYS CFX12.0®. The temperature profiles, calculated numerically on the base and on the top of the fin, were compared with the experimental temperatures and the maximum difference was lower than 2%.*

Keywords*: Heatsinks, Convection Heat Transfer Coefficient, Natural Convection, CFX, Experimental and Numerical Methods.*

1. INTRODUCTION

The use of fin surfaces increases the rate of heat transfer between hot surfaces and certain fluids through an increase in contact area between them. The fins are used in several devices, mainly in electronics. Each year, a new generation of powerful and more compact equipment is developed, which, in turn, need new heatsinks to keep them at operating temperatures. Natural convection is usually used because it presents high reliability and lower cost and does not use energy. The selection of the heatsink is done in accordance with the rate of heat dissipated. This rate can be calculated by knowing the convection heat transfer coefficient which is a property that depends on the fluid flow conditions and the geometry of the surface. The values of $\bar{h}$ can be found by resorting to experiments, numerical solutions and empirical correlations.

Venkateshan and Rao (1996) focused their studies on the influence of the portion related to radiation in predominantly convective processes and methods of obtaining this portion. The authors stated that the portion of the radiation fins in case of reduced height, low emissivity and good finish, can be neglected. A study of the influence of the orientation and density of the fins, with natural convection in the performance of heatsinks was performed by Huang et al. (2006). They tested six heatsinks, four with pin-shaped blades and 2 with rectangular fins, in horizontal, vertical and horizontal inverted positions. It was observed that the coefficient of heat transfer by convection increases with the increase of the contact area up to a certain density of fins, thereafter it decreases. Furthermore, the authors noted that $\bar{h}$ is greater for the horizontal orientation, followed by the vertical orientation and the smallest value for inverted horizontal orientation for pin-shaped fin heatsinks. Whereas for the rectangular fins heatsinks a larger $\bar{h}$ was observed for vertical orientation followed by horizontal and inverted horizontal orientations. This difference in the results was explained by the different flow patterns around the different heatsinks. The authors also presented various experimental values of $\bar{h}$ and concluded that pin-shaped fin heatsinks generally have better performance than rectangular fin ones. An experimental study on the effect of spacing between fins, fin height and magnitude of heat flow on heat transfer by convection was conducted by Dogan and Sivrioglu (2009). Thus, a rectangular fin heatsink in a horizontal position was placed inside a controlled air flow channel. The authors observed a range where the optimal value for the dimensionless spacing between fins depends on the Rayleigh number and size of the fin.

The material of the fins must display high thermal conductivity. In the present work, aluminum 6063-T5 was used. The material of the fin has great influence on the heat transfer rate, since it affects directly the temperature distribution along the extended surface. The optimal configuration would occur if the thermal conductivity of the fin was infinite, thus the temperature along the fin would be the same as the base, providing a maximum rate of heat transfer.

In this study, the average coefficients of convection heat transfer of six heatsinks were determined. These values were compared with the empirical correlation obtained by Harahap and Rudianto (2005). In some cases the differences were less than 5%. Another important analysis performed was the behavior of the heat flow due in function of temperature variation. This analysis was carried out analogously to Harahap and Rudianto (2005) and Huang *et al.* (2006). Simulations with the commercial software ANSYS-CFX12.0® were carried out. The numerical temperatures obtained at the same positions where the thermocouples were placed were compared with the experimental ones. The final temperatures encountered during the steady state were compared and the differences were less than 2%. This study can be used, in future work, in order to analyze whether or not the effect of thermal paste used experimentally presents any influence on the results.

2. EXPERIMENTAL ASSEMBLY

The experimental apparatus illustrated in Fig. 1a was developed to conduct the tests. The heatsink is mounted on a resistive heater and both are mounted on a wood support as shown in Fig. 1b. This assembly reduces heat loss through the lower surface of the heater and provides no restriction to air flow around the peripheral fins. The sidewalls of the support were isolated with glass wool to prevent heat exchange between the support and the heatsink. Additionally, a medium density fiberboard, commercially known as MDF, was used to isolate the bottom of the heater to avoid buckling and to keep it in contact with the base of the heatsink. A layer of silver thermal paste (Arctic Silver 5) was applied on the heater to aid heat conduction to the heatsink.

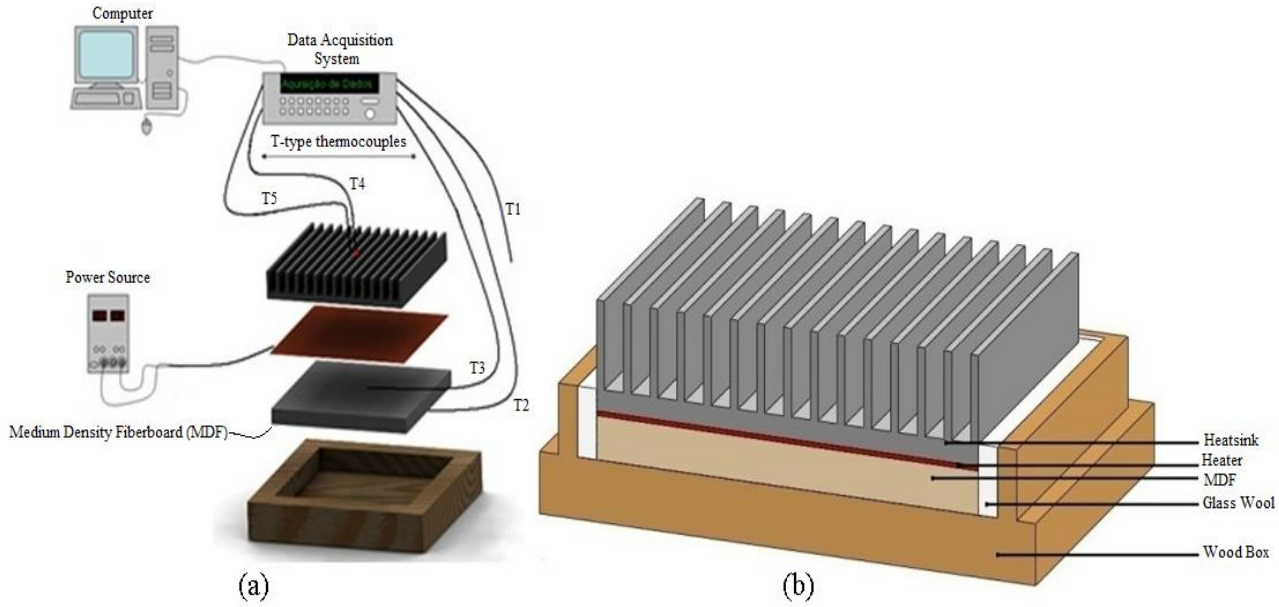

Figure 1. (a) Arrangement of test bench and (b) details of the heatsink.

The heater was connected to a source of Instrutemp ST-II-305D DC power supply with the digital current and voltage display. The six heatsinks with different geometrical parameters and the same base were machined from a homogeneous 6063-T5 aluminum bar at the Machining Laboratory of UNIFEI. 6063-T5 aluminum was chosen due to its wide use in heatsinks and the fact of presenting high thermal conductivity and low density, which are essential characteristics for heatsinks. Another important factor was its affinity with the capacitive discharge welding, a process used to attach the thermocouples directly to the heatsinks.

Five T-type thermocouples were used in the assembly. The capacitive discharge welding (Vilarinho, 2003) was used because it reduces the contact resistance between the thermocouple and the heatsink. The thermocouples were connected to a data acquisition system, Agilent 34980A, controlled by a computer that recorded temperatures in a data file.

The dimensions of the heatsinks are shown in Tab. 1.

The geometrical parameters of the heatsinks are shown in Fig. 2b and the MDF board, Fig. 2c. Dimensions of the heatsinks and MDF board are shown respectively in Tab. 1 and Tab. 2. The MDF board 1 was used with Heatsinks 2, 5 and 6; and MDF 2 was used with Heatsinks 1, 3, and 4.

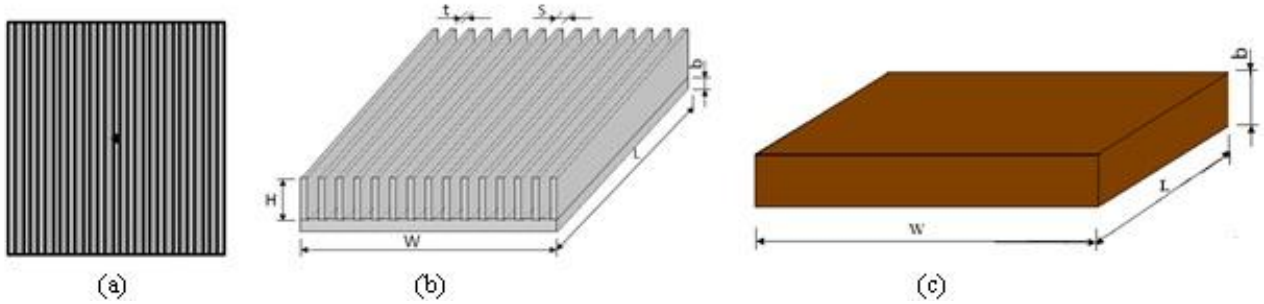

Figure 2. (a) Position of thermocouples on the heatsinks (obtained from Naia *et al.* (2008)), (b) geometrical parameters of the heatsink and (c) geometrical parameters of MDF board.

Table 1. Dimensions of the heatsinks.

	n	**S [mm]**	**t [mm]**	**H [mm]**	**L [mm]**	**W [mm]**	**b [mm]**
Heatsink	Number of fins	Fin spacing	Thickness	Height	Length	Width	Base plate thickness
1	7	14,35	2,00	7,00	100,00	100,10	4,00
2	7	14,35	2,00	14,00	100,00	100,10	4,00
3	7	14,35	2,00	20,00	100,00	100,10	4,00
4	14	5,55	2,00	7,00	100,00	100,15	4,00
5	14	5,55	2,00	14,00	100,00	100,15	4,00
6	14	5,55	2,00	20,00	100,00	100,15	4,00

Table 2. Dimensions of MDF board 1 and 2.

Dimension	**Average value for MDF 1 [mm]**	**Average value for MDF 2 [mm]**
L	100,17	110,00
W	99,97	111,02
B	15,00	18,40

3. THEORETICAL BASIS

3.1 Calculation of the Mean Convection Heat Transfer Coefficient

The heat transfer by free convection occurs whenever there is a temperature difference between a body and a fluid. This difference in the temperature causes a change in the density of the fluid near the surface. The difference in density means that there is a downward flow of the heavier fluid and an upward flow of the lighter one. The convective heat transfer that occurs due to the difference between the densities of the fluid is called natural convection.

The theoretical coefficients obtained in this work were based on empirical correlations proposed by Harahap and Rudianto (2005). The correlations are obtained from a series of tests for assessment of experimental data. The accuracy with which the heat transfer coefficient can be calculated depends on the correlation used.

Natural convection is characterized by the dimensionless numbers of Nusselt, Grasshof, Prandtl and Rayleigh. The Nusselt number represents the ratio between the heat transfer by convection and by conduction. Grasshof number indicates a ratio of the buoyant forces and the viscous forces, and Prandtl number represents the ratio between the momentum and thermal diffusivities. The dimensionless numbers can be calculated by using the equations below:

$$Gr = g\beta(T_5 - T_\infty)/\nu^2 \quad (1)$$

$$Nu = hl / k_f \quad (2)$$

$$Pr = \upsilon / \alpha \quad (3)$$

$$Ra = Gr.Pr \quad (4)$$

$$l = L/2 \quad (5)$$

In these equations, L is the width of the heatsink, g is the acceleration of gravity, β is the thermal coefficient of volumetric expansion, T_s is the temperature on the heatsink surface, υ is the kinematic, k_f is the thermal conductivity of the fluid and α is the thermal diffusivity of the fluid.

3.1.1 Empirical correlation of Harahap e Rudianto (2005)

Harahap and Rudianto (2005) proposed a correlation to describe natural convection in horizontal finned rectangular heatsinks. The correlation proposed by these authors uses Rayleigh and Nusselt numbers calculated in relation to the size of *l*, where *l = L/2*. Thus, Nusselt number is calculated from the equation below:

$$Nu = 0{,}203[Gr.Pr\ (n.S/H)]^{0{,}393}\ (S/l)^{0{,}470}\ (H/l)^{0{,}870}\ (L/W)^{0{,}620} \tag{8}$$

and the mean value of the coefficient of heat transfer by convection is given by:

$$\bar{h} = (Nu.k_f) / l \tag{9}$$

The correlation obtained by Harahap and Rudianto (2005) is indicated for a range of values between $3\text{x}10^3 \leq Ral_n\ (S/L) \leq 3\text{x}10^5$. The use of this correlation for values outside the indicated range increases the error of the values obtained for $\bar{h}$.

3.1.2 Calculation of Heat Lost Through Insulation

The lost heat transfer rate by conduction through the insulation used in the assembly can be calculated by Fourier's Law:

$$q = -\,k.A.\,dt/dx = k.A.\,(T_3\text{-}T_2)/b \tag{10}$$

where k is the thermal conductivity of the insulating material, A is the surface area of the insulator, T_2 and T_3 are respectively the temperatures of upper and lower insulator and b is the distance between the two surfaces considered Fig. 2c. The value adopted for the thermal conductivity of 0.14 W/mK for the MDF used as insulation was removed from Lienhard IV and Lienhard (2006).

3.1.3 Obtaining the experimental $\bar{h}$

To obtain the experimental values of $\bar{h}$, Newton`s cooling law was used, given as:

$$\bar{h} = q_{pl}/\left[A_{ct}\left(T_s\text{-}T_\infty\right)\right] \tag{11}$$

where A_{ct} is the total surface area of the heatsink in contact with the fluid, q_{pl} is the difference between the rate of heat transfer provided by the heater and lost by conduction through the insulator. The amount of heat transferred through radiation was neglected due to the low emissivity of the material of the heatsinks and the small temperature differences between these and the environment (Rao and Venkateshan, 1996).

3.2 Calculation of temperature on the fin

To compute the temperature distribution along height H of the fin, admitting a uniform fin, the following expression is used (Incropera and DeWitt, 1998):

$$\theta/\theta_b = \left[\cosh m\left(H\text{-}x\right)+(\bar{h}/m.k)\sinh m\,(H\text{-}x)\right]/\left[\cosh m.H+(\bar{h}/m.k)\sinh\,(m.H)\right] \tag{12}$$

where θ is the difference between the temperature at a distance x along H and the room temperature, θ_b is the difference between the substrate temperature and room temperature, m is expressed in Eq. (13) and H is the height of the fin.

$$m^2 = \bar{h}P/kA_{sr} \tag{13}$$

In Equation (13), P is the perimeter of the fin and A_{sr} is the cross-sectional area of the fin.

3.3 Simulation in ANSYS-CFX 12.0®

To accomplish the simulation on ANSYS–CFX 12.0® the geometry that represents the heatsink to be simulated was built in ICEM CFD®. Then the blocking step which guides the mesh formation is started, Fig. 3a. After that, a hexahedral mesh is generated with the appropriate refinement to the problem. Finally the mesh is imported by the program CFX. In CFX, the other parameters are attributed to this geometry like the boundary conditions, such as imposed heat flux and others, as shown in Fig. 3b. Thermophysical properties were obtained from Lienhard IV and Lienhard (2006) and are presented in Tab. 2 while the not shown values in the Tab. 2 were obtained by interpolation.

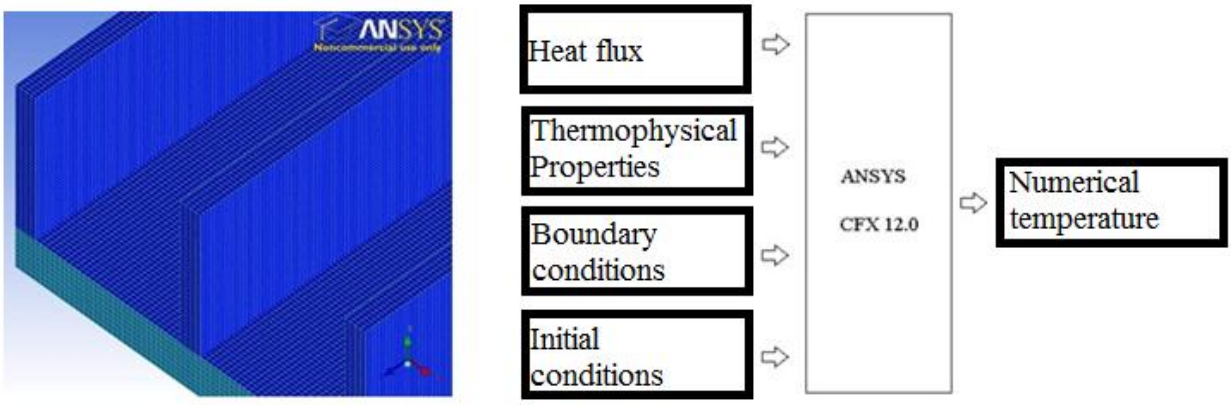

(a) (b)

Figure 3. (a) Mesh used and (a) ANSYS operations flowchart.

Table 3. Thermophysical Properties of air at atmospheric pressure.

T(K)	ν (m^2/s)	k (W/m.K)	α (m^2/s)	Pr
300	0,00001578	0,02623	0,00002213	0.713
310	0,00001659	0,02684	0,00002340	0.709
320	0,00001754	0,02753	0,00002476	0.708
330	0,00001852	0,02821	0,00002616	0.708
340	0,00001951	0,02888	0,00002821	0.707

4. RESULTS

In Figures 4-6 the comparison between experimental values of $\bar{h}$ for the six heatsinks configurations are presented. Five experiments were conducted for each temperature range. The expected behavior is that the value of $\bar{h}$ increases as the temperature difference between the heatsink and the environment increases. This behavior is observed in all the heatsinks (Figs. 4-6).

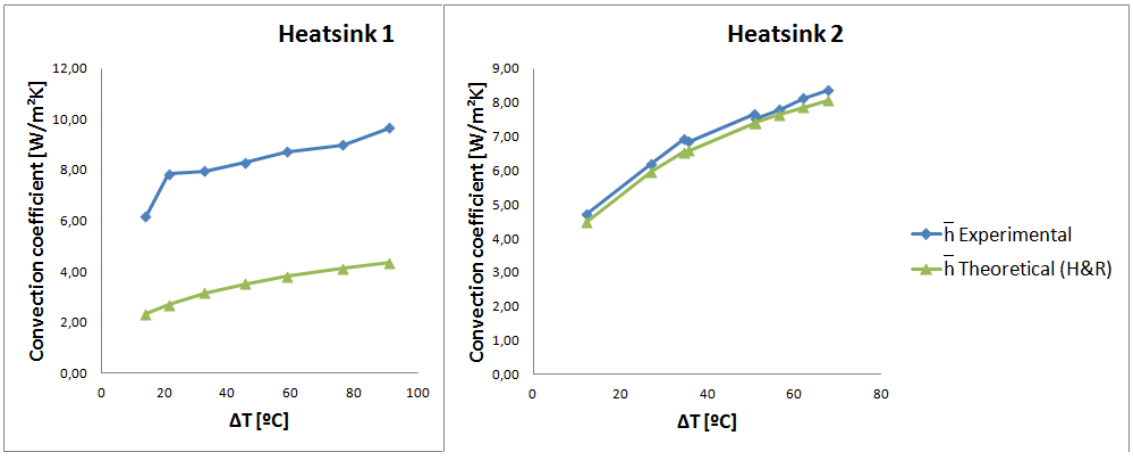

Figure 4. Values of $\bar{h}$ in relation to ΔT for Heatsink 1 and 2.

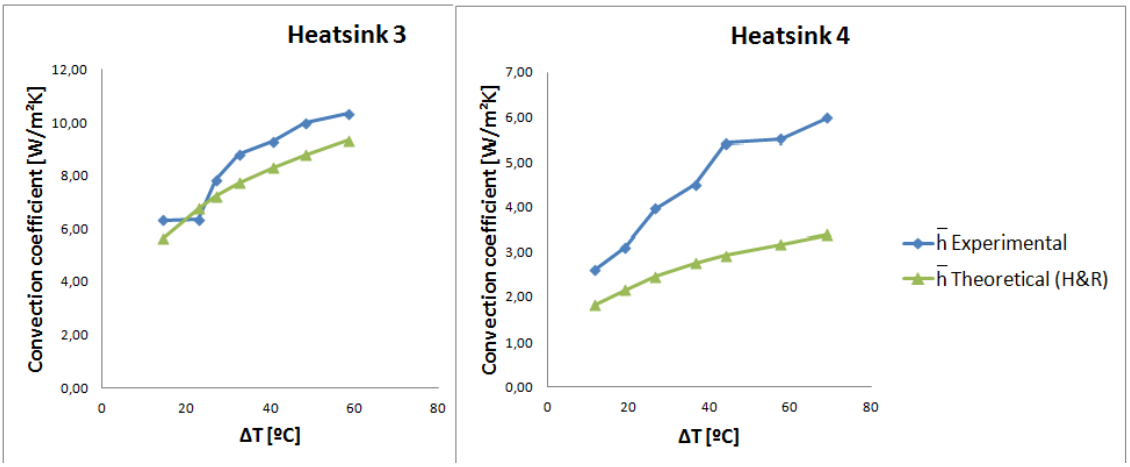

Figure 5. Values of $\bar{h}$ in relation to ΔT for Heatsink 3 and 4.

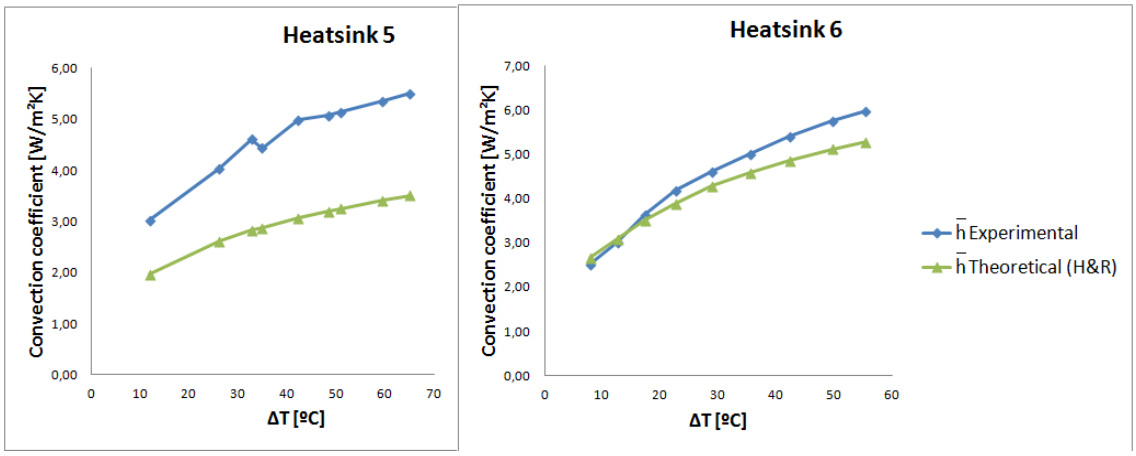

Figure 6. Values of $\bar{h}$ in relation to ΔT for Heatsink 5 and 6.

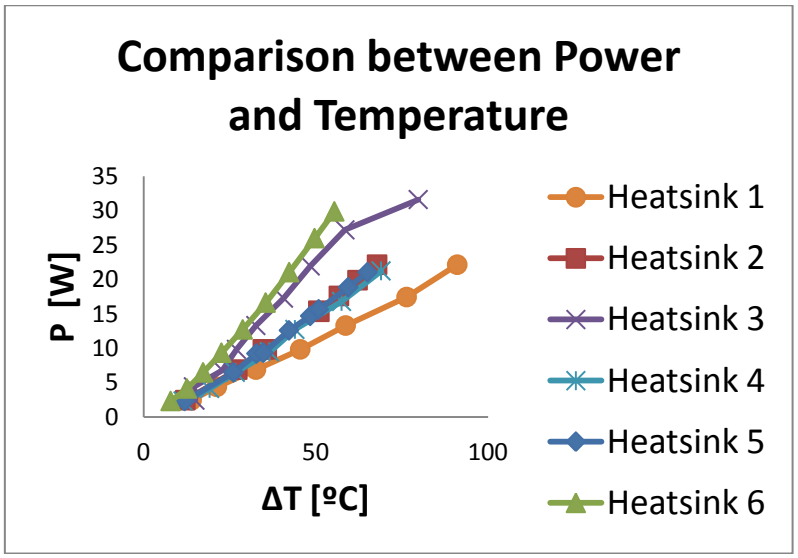

Figure 7. Power supplied as function of ΔT, for each heatsink

In Figure 7 values of power supplied by the resistive heater for each corresponding ΔT is described. Thus the order of efficiency could be written as: Heatsinks 6, 3, 5, 2, 4 and 1.

The computational results presented small differences when compared with the experimental values of temperatures for the same flow conditions. The small difference between the final temperatures found in the experiment and those found in the simulation by using CFX can be verified in Tab. 4. This difference may decrease if the effect of thermal paste is included in the numerical simulations.

Figure 8 shows the temperature fields obtained through CFX for Heatsinks 2 and 5. This figure illustrates the uniform temperature distribution. The numerical results were obtained using a single computer with a Intel ® Core ™ 2 Quad 2.40 GHz processor, 8GB of RAM memory. All the simulations took approximately 12 hours.

Table 4. Final temperature for thermocouple 4 in steady state.

Heatsink	Heat Flux [W/m^2]	Temperature [ºC]		
		Experimental	Simulation	Analytical
2	2692	105,35	105,84	107.83
5	2683	111,42	110.13	110.93

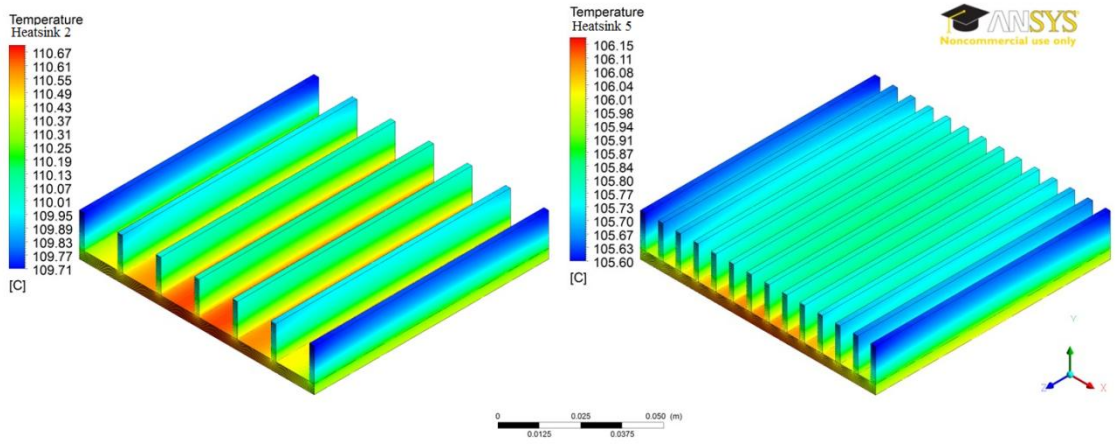

Figure 8. Temperature field in Heatsinks 2 and 5.

4. CONCLUSIONS

A good agreement with the values of Harahap and Rudianto (2005) correlation was observed when comparing the results of $\bar{h}$ obtained in this study. In some cases the maximum difference of $\bar{h}$ was less than 5%. These differences probably happened due to the fact that for these heatsinks the Rayleigh number values in this work were out of the range proposed by Harahap and Rudianto (2005). Heatsink 2 showed the best results for $\bar{h}$, with a difference less than 2%. Similar behavior was obtained for Heatsinks 3 and 6.

It was observed that heatsink 6 greatest the heat dissipation due to its geometrical characteristics. It has largest area of heat exchange, largest height and number of fins among the heatsinks used.

The temperature values obtained with thermocouple 4 were compared to the numerical results just for Heatsinks 2 and 5. The reason is that for these heatsinks there was a small difference of the values. Maybe it will be possible to improve these results including the thermal paste effect on the numerical simulation.

5. ACKNOWLEDGEMENTS

The authors would like to thank CNPq, FAPEMIG and CAPES for their financial support. The authors would also like to thank Zilma Moura de Castro for checking and improving the English of this paper.

6. REFERENCES

Dogan, M., Sivrioglu, M., 2009 “Experimental Investigation of Mixed Convection Heat Transfer from Longitudinal Fins in a Horizontal Rectangular Channel: In Natural Convection Dominated Flow Regimes”, Energy Conversion and Management, Vol. 50, pp. 2513- 2521.

Harahap, F., Rudianto, E., 2005, "Measurements of Steady-State Heat Dissipation From Miniaturized Horizontally Based Straight Rectangular Fin Arrays", Heat and Mass Transfer, Vol.41, pp. 280-288.

Huang, R.T., Sheu, W.J., Wang, C.C., 2006, "Natural Convection Heat Transfer From Square Pin Fin and Plate Fin Heat Sinks Subject to the Influence of Orientation", 13th International Heat Transfer Conference – IHTC13, Sydney, Australia.

Incropera, F.P., DeWitt, D.P., 1998, "Fundamentos de Transferência de Calor e Massa" LTC – Livros Técnicos Científicos S.A., 4º ed., Rio de Janeiro, Brasil, 494 p.

Lienhard IV, J. H., Lienhard V, J. H., 2006, "A Heat Transfer Textbook", Phlogiston Press., 3º ed., Cambridge, Massachusetts.

Naia, F. R., Lima e Silva, A. L. F., Lima e Silva, S. M. M., 2008, "Análise da Transferência de Calor por Convecção Natural em Aletas Planas Retangulares", V CONEM (Congresso Nacional de Engenharia Mecânica), Salvador, Bahia, Brasil.

Rao, V.R., Venkateshan, S.P., 1996, "Experimental Study of Free Convection and Radiation in Horizontal Fin Arrays", International Journal of Heat Mass Transfer, Vol. 39, pp 779–789.

Vilarinho, L. O., 2003, "Desenvolvimento de Técnicas Experimentais e Numéricas para a Caracterização de Arcos TIG", Tese de Doutorado, Universidade Federal de Uberlândia, Uberlândia. MG, Brasil, 218 p.

7. RESPONSIBILITY NOTICE

The authors are the only responsible for the printed material included in this paper.